ELSEVIER

Polymer 42 (2001) 1995–2000

polymer

www.elsevier.nl/locate/polymer

Structural and morphological changes and polymerization behaviors of diacetylene Langmuir–Blodgett films on adding water-soluble polyallylamine in the subphase

H. Tachibana[a,*], Y. Yamanaka[b], H. Sakai[b], M. Abe[b], M. Matsumoto[a]

[a]*National Institute of Materials and Chemical Research, 1-1 Higashi, Tsukuba 305-8565, Japan*
[b]*Science University of Tokyo, Noda 278-8510, Japan*

Received 16 June 2000; received in revised form 7 July 2000; accepted 28 July 2000

Abstract

Langmuir–Blodgett (LB) films of an amphiphilic diacetylene (DA) were fabricated from the aqueous subphase where a water-soluble polymer, polyallylamine (PAA), was added by varying the concentrations. The effect of the PAA concentration on the structure, the morphology, and the polymerization in the DA/PAA LB film was investigated by measurements of XPS and IR spectra, atomic force microscopy (AFM), and the UV-visible absorption spectral changes on irradiation with UV light, respectively. The component ratio between DA and PAA and the ionic states of the components changed with the concentrations. The morphology and the polymerization behaviors depend strongly on the component ratio. At PAA concentration of 0.1 mM, nanofibers with a width of 30 nm and a height of 2 nm were observed in the DA/PAA LB films. We have demonstrated that globular structures form the nanofiber structures.

Keywords: Langmuir–Blodgett films; Polyion complex; Nanofibers

1. Introduction

Langmuir–Blodgett (LB) technique is highly advantageous from the viewpoint of fabricating highly ordered structures at the molecular level [1–3]. Usually, amphiphilic molecules are used for this purpose. When the monolayers at the air–water interface are not stable enough or are not transferred easily onto solid substrates, polyion complex method coupled with the LB technique is employed [4–16]. This method utilizes the electrostatic interaction between the amphiphiles spread at the air–water interface and the water-soluble polyions added in the subphase. This method has been also used to fabricate the organic–inorganic alternate-layered LB films [17–21]. The important aspect of the polyion complex method is that the structures and properties of the hybrid monolayers can be controlled by the polyion species. In this respect, we have observed that photoisomerization of azobenzene in the polyion complex LB films depends strongly on the polyion species [11,16]. Furthermore, we have also found that the morphology can be controlled by the *cis–trans* photoisomerization of azobenzene in the polyion complex LB films [13].

In this paper, we describe the fabrication of the LB films of an amphiphilic diacetylene (DA) from a subphase where a water-soluble polymer, polyallylamine (PAA), was added by changing the concentration of PAA. The effect of concentration on the structures of the LB films were characterized using XPS and FT-IR spectroscopies, with special emphasis on the component ratio and the ionic states of the components. In order to obtain further information on the morphology and the polymerization of the DA/PAA LB film fabricated at various concentrations of PAA, atomic force microscopy (AFM) and UV–Visible absorption spectra were measured, respectively.

2. Experimental section

2.1. Materials

10,12-Pentacosadiynoic acid (DA) was synthesized by following the procedures in the literature [22]. Polyallylamine (PAA; $M_W = 1 \times 10^4$) was obtained from Nittobo Corp. UV spectroscopic grade chloroform was purchased from Dojin. The water used in this study was purified by distilling deionized water after passing it through a milli-Q

* Corresponding author. Tel.: +81-298-61-4668; fax: +81-298-61-4669.
E-mail address: htachibana@nimc.go.jp (H. Tachibana).

0032-3861/01/$ - see front matter
PII: S0032-3861(00)00579-6

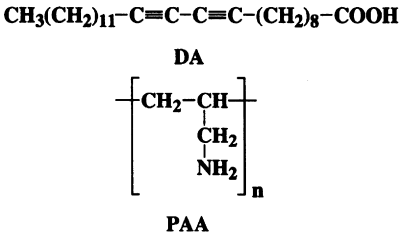

Fig. 1. Molecular structures used in this study.

filter. The molecular structures used in this study are shown in Fig. 1.

2.2. Monolayer formation and LB film deposition

Surface pressure–area (π–A) isotherms were obtained using a Lauda Film balance. Chloroform solution of DA was spread at 17°C on the subphase with a given concentration of PAA_{unit}, where PAA_{unit} is the monomer unit of PAA. Monolayers were transferred at a surface pressure of 25 mN m^{-1} onto the substrates by the horizontal lifting method, otherwise the target surface pressure is indicated.

2.3. Characterization

XPS spectra were obtained on a Perkin–Elmer PHI 5600ci ESCA system with monochromated Alkα radiation. Measurements of the LB films on glass substrates were carried out with a resolution of 1.8 and 0.4 eV for the overall and narrow scan, respectively, with a take-off angle of 45°. Binding energies were calibrated by referring to the aliphatic C1s line at 284.5 eV. The infrared spectra were obtained with a Perkin–Elmer Spectrum 2000 FTIR. Reflection–absorption (RA) spectra of LB films on gold substrates were measured at an incident angle of 80°. A Seiko SPA300 atomic force microscope, operating a noncontact mode, was employed to image the morphology of a single-layer LB film on mica. The AFM image was obtained at line scan rates of 1 Hz, using silicon cantilevers with a resonance frequency of 28 kHz and a spring constant of 1.9 mN m^{-1}.

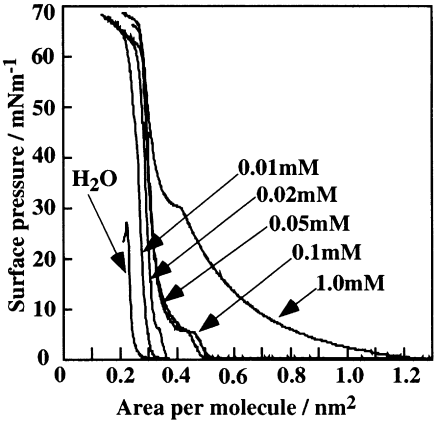

Fig. 2. Surface pressure–area isotherms of DA at 17°C on aqueous subphases containing various concentrations of PAA_{unit}; 0.01, 0.02, 0.05, 0.10 and 1.00 mM, and on a pure water subphase.

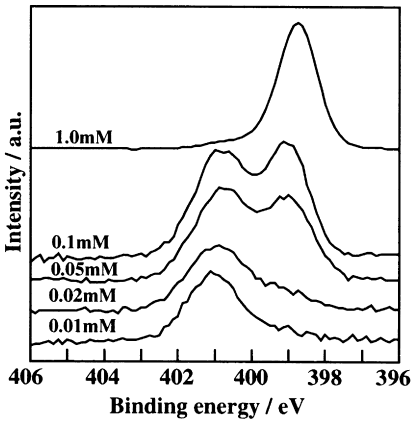

Fig. 3. N1s region of the XPS spectra of the 10-layer DA/PAA LB films at various PAA_{unit} subphase concentrations: 1.00, 0.10, 0.05, 0.02 and 0.01 mM.

2.4. Irradiation

The UV–Visible spectra were measured with a Shimazu UV-265FS spectrometer. The LB film was placed on a rotating table and was irradiated with UV light for various times. A 50 W low-pressure mercury lamp was used as the source of UV light for the polymerization. The distance between the Hg lamp and the film surface was 20 cm.

3. Results and discussion

3.1. Surface pressure–area isotherm

Fig. 2 shows the π–A isotherms of DA with varying concentrations of PAA_{unit} in the subphase. For comparison, the π–A isotherm of DA on pure water is also shown. The addition of PAA in the subphase has two effects: one is the increase in the collapse pressure, and the other is the increase in the area per molecule. The former suggests that the monolayer is stabilized by the presence of PAA. The latter becomes more prominent with increasing concentration of PAA in the subphase. These results will be reconciled if we assume that DA in the monolayer at the air–water interface has an electrostatic interaction with PAA in the subphase, and forms polyion complex monolayers with PAA. The fact that the isotherm depends on the PAA_{unit} concentration in the subphase suggests that the composition of the LB films changes with the PAA_{unit} subphase concentration. The LB films of DA fabricated from the subphase containing PAA will be referred to as DA/PAA LB films hereafter.

3.2. Structure

In order to investigate the structures of the DA/PAA LB

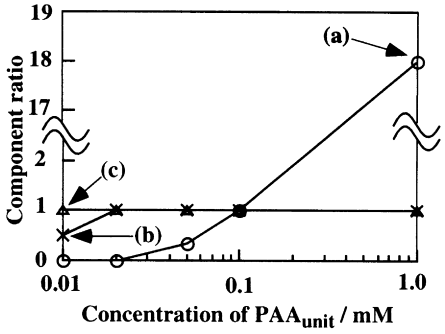

Fig. 4. Component ratio in DA/PAA LB films as a function of PAA_{unit} subphase concentration. (a) $r(PAA^0_{unit}/DA_{total})$, (b) $r(PAA^+_{unit}/DA_{total})$, (c) $r(PAA^+_{unit}/DA^-)$.

films, we measured the XPS spectra of the LB films. Fig. 3 shows the variations in the N1s region of the XPS spectra of the 10-layer DA/PAA LB films on changing the concentration of PAA_{unit} in the subphase. When the PAA_{unit} concentration is 0.01 mM, an intense band is evident at ca. 401 eV, which is assigned to the +1 state of N1s emission originating from the PAA molecules [4,23]. This shows that all the PAA molecules are protonated in the LB films at this PAA_{unit} subphase concentration. When the PAA_{unit} subphase concentration is increased, another band appears at an energy lower than 401 eV, which is assigned to the neutral state of nitrogen in PAA [4,23]. This band becomes more prominent with an increasing PAA_{unit} subphase concentration.

The component ratio of PAA^0_{unit} to DA_{total}, $r(PAA^0_{unit}/DA_{total})$, where DA_{total} is the sum of the neutral and anionic forms of DA in the LB films, is obtained by integrating the areas of N1s band in the neutral state and C1s band, followed by appropriate calculations. Similarly, the component ratio of PAA^+_{unit} to DA_{total}, $r(PAA^+_{unit}/DA_{total})$, in the LB films is obtained by integrating the areas of N1s band in the +1 state and C1s band. The plot of these ratios is shown in Fig. 4. It is clear that more and more PAA molecules in the neutral state are incorporated in the LB films when the PAA_{unit} concentration in the subphase increases.

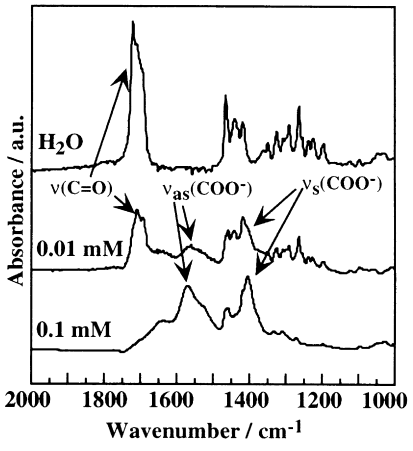

Fig. 5. Infrared reflection–absorption (RA) spectra of 10-layer DA/PAA LB films at PAA_{unit} subphase concentrations of 0, 0.01 and 0.1 mM.

Infrared spectroscopic analyses of the LB films give us important information on the ionic state of the carboxylic group. Fig. 5 shows the infrared RA spectra of the 10-layer DA/PAA LB films at the PAA_{unit} subphase concentration of 0.01 and 0.1 mM. For comparison, the RA spectra of DA LB films on pure water are also shown in Fig. 5. At PAA_{unit} subphase concentrations of more than 0.01 mM, two bands were observed in the C=O stretching region. These bands, located at 1407 and 1571 cm^{-1}, were assigned to the symmetric ν_s (COO^-) and the asymmetric (ν_{as} (COO^-)) stretching modes of the COO^- group, respectively [24,25]. This shows that all the DA molecules are deprotonated (DA^-) in this region. On the other hand, at a PAA_{unit} subphase concentration of 0.01 mM, three bands appeared in the C=O stretching region. The additional band located at 1720 cm^{-1} was assigned to the C=O stretching mode of the carboxylic group [24,25]. From the analysis of the intensity of each band, it is concluded that one half of the DA molecules are in the neutral state (DA^0) and that the other half are deprotonated.

By combining the results of XPS and IR measurements, we estimated the component ratio of PAA^+_{unit} to DA^-, $r(PAA^+_{unit}/DA^-)$, the plot of which is shown in Fig. 4. It is clear that this value is almost unity irrespective of the PAA_{unit} subphase concentration. This means that the charge is balanced in the LB films by considering only the above-mentioned species, DA^0, DA^-, PAA^0_{unit}, and PAA^+_{unit}. This suggests that DA^- and PAA^+_{unit} form salt in the LB films. Two types of DA species, DA^- complexed with PAA^+_{unit} and DA^0, are present in the LB films at a PAA_{unit} subphase concentration of 0.01 mM while only the DA^- species is present in the LB films at higher PAA_{unit} subphase concentrations. This is due to the increasing pH values with increasing PAA_{unit} concentration in the subphase: pH of the subphase was equal to 6.00, 6.30, 6.75 and 9.05 for a PAA_{unit} subphase concentration of 0.01, 0.05, 0.10 and 1.00 mM, respectively. At higher PAA_{unit} subphase concentrations, DA^0 is absent and instead PAA^0_{unit} is present in addition to PAA^+_{unit} in the LB films. The incorporation of the PAA^0_{unit} species in the LB films suggests that this species is physically adsorbed under and/or within the DA^-/PAA^+_{unit} monolayers. This is the reason for the expansion of the π–A isotherms at higher PAA_{unit} subphase concentrations.

These results indicate that the change in the concentration of PAA_{unit} in the subphase plays an important role in determining the component ratio of PAA_{unit} to DA in the LB films. The addition of PAA in the subphase has several effects. First, PAA forms polyion complex with DA due to salt formation. Second, pH of the subphase depends on the concentration of PAA_{unit}. Finally, the neutral form of PAA is

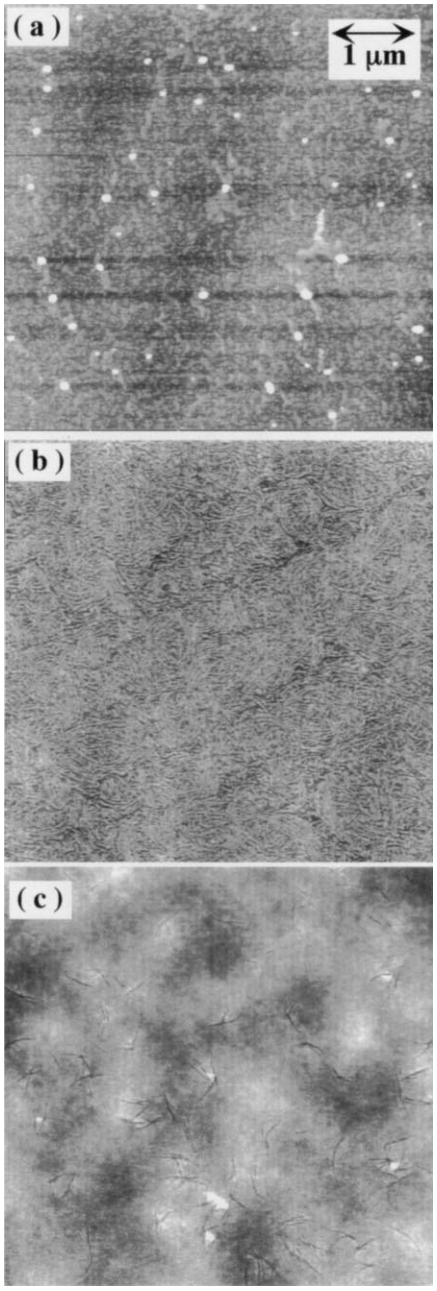

Fig. 6. AFM images (5 μm × 5 μm) of a single-layer LB film at three kinds of PAA_{unit} subphase concentrations: (a) 0.01 mM, (b) 0.1 mM, (c) 1 mM.

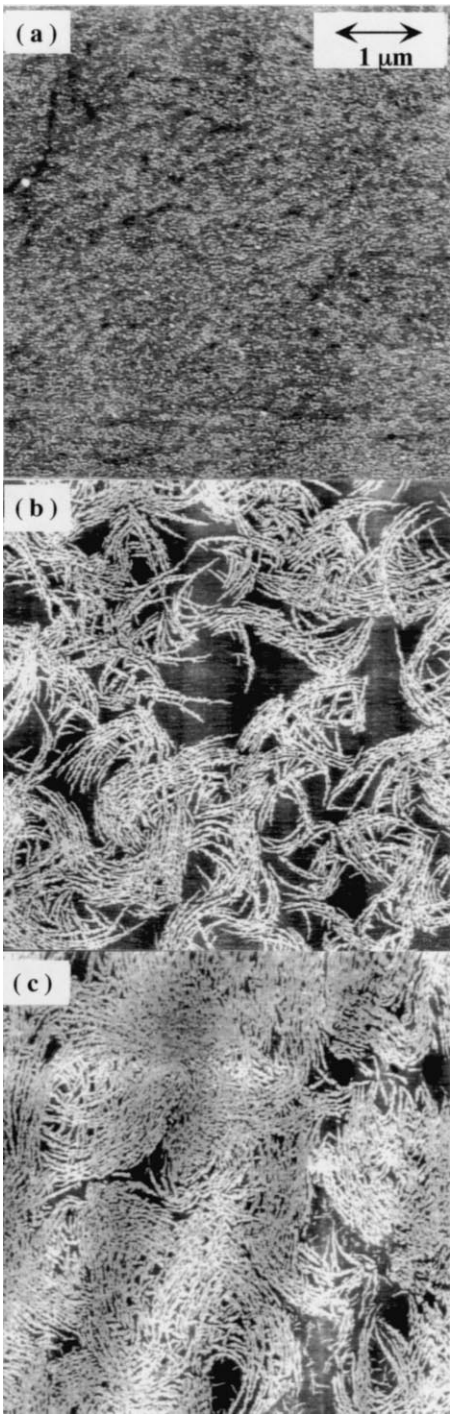

Fig. 7. AFM images (5 μm × 5 μm) of a single-layer LB film transferred at different surface pressures: (a) 5 mN m^{-1}; (b) 8 mN m^{-1}; (c) 15 mN m^{-1}.

also incorporated in the LB films due to physical adsorption at higher PAA_{unit} subphase concentrations.

3.3. Morphology

The morphology of a single-layer DA/PAA LB film was investigated using atomic force microscopy (AFM). Fig. 6 shows the AFM image of the DA/PAA LB film for three kinds of PAA_{unit} subphase concentrations, 0.01, 0.1 and 1 mM. The morphology is sensitive to the PAA_{unit} subphase concentration. When the PAA_{unit} subphase concentration is 0.01 mM, the DA/PAA LB film is not homogeneous. In addition, the globular structures are found on the surface. An increase in the PAA_{unit} subphase concentration yields a smoother film, though the globular structures are observed on the surface. Since DA^0 eventually disappears with increasing the PAA_{unit} subphase concentration in the DA/PAA LB film, the heterogeneous structures are probably composed of DA^-/PAA^+ complex-rich phase and DA^0-rich one. On the other hand, the AFM images at a higher

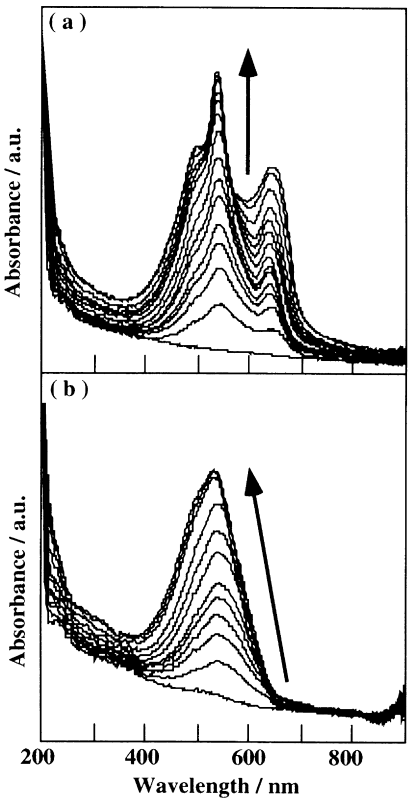

Fig. 8. Change in UV–Visible absorption spectra of 10-layer DA/PAA LB films at: (a) 0.01 mM and (b) 0.1 mM on irradiation with UV light.

PAA_{unit} subphase concentration (1 mM) exhibit spongy morphology with a few cracks as shown in Fig. 6(c).

At the PAA_{unit} subphase concentration of 0.1 mM, the morphology changes drastically as shown in Fig. 6(b). The AFM image shows a fingerprint-like pattern, which consists of many nanofibers with an average width of 30 nm and an average height of 2 nm. These nanofiber structures are not observed in AFM images of the DA/PAA LB films at the other PAA_{unit} subphase concentrations. Furthermore, the nanofiber structures were not observed in the AFM image of a single-layer LB film of arachidic acid complexed with PAA fabricated at the same concentration. These results indicate that two factors, $\pi-\pi$ interaction between butadiyne groups and the component ratio between DA and PAA_{unit}, play an important role in the formation of the nanofiber structures in the DA/PAA LB films.

3.4. Effect of preparation conditions on nanofiber formation

We investigated the effect of the preparation conditions on the formation of nanofibers in the DA/PAA LB film fabricated at the PAA_{unit} subphase concentration of 0.1 mM. The size of the nanofibers was the same irrespective of the preparation conditions such as the concentration of the spreading solution, the kind of the solvent, the subphase temperature, and the dipping speed. To clarify the formation of nanofibers, we investigated the morphology in the DA/PAA LB film transferred at various surface pressures. Fig. 7 shows the AFM images of the single-layer DA/PAA LB film transferred at three different surface pressures (5, 8 and 15 mN m^{-1}) onto a freshly cleaved mica. Many globules with a diameter of 30 nm are observed in AFM images of the LB film transferred before the deflection point at 5 mN m^{-1} (Fig. 7(a)). It is clear that all the surfaces are covered with the globules of the same diameter of same size. Fig. 7(b) shows the AFM images of DA/PAA LB film transferred just after the deflection point at 7 mN m^{-1}. Twig-like nanofibers gather together to form nest-like structures. These nanofibers have an average width of 30 nm and an average height of 2 nm. Each nanofiber has several intersections. When the transfer pressure increases, the number of the nanofibers and the nest-like structures increased. Furthermore, the nest-like structures became larger and gathered more tightly. This suggests that the nanofibers are formed by the participation of more and more globules at the ends of the nanofibers. At more higher surface pressure, each nest-like structure is compressed to form a fingerprint-like pattern (Fig. 7(c)). The average width and height of the nanofibers do not change significantly during the compression after the deflection point. Finally, the nanofibers become more closely each other.

3.5. Polymerization behavior

The effect of the PAA_{unit} subphase concentration on polymerization behaviors in the DA/PAA LB films was investigated by measurements of UV–Visible spectra on irradiation with UV light. Polymerization behaviors can be classified into two groups, depending on the PAA_{unit} subphase concentrations, the component ratio of PAA_{unit} to DA_{total} ($r(PAA_{unit}/DA_{total})$). A typical spectral change of the DA/PAA LB films belonging to group I is shown in Fig. 8(a). Two absorption bands appear at 540 and 630 nm simultaneously on irradiation with UV light, which correspond to red and blue phase, respectively. On prolonged irradiation, only the intensity of both bands grows gradually without any noticeable changes in spectral features and absorption shifts. The DA/PAA LB films with $r(PAA_{unit}/DA_{total})$ less than one belong to this group I. From the above-mentioned spectroscopic results, it is clear that the two types of DA species, DA^- complexed with PAA^+_{unit} and neutral state of DA^0 without PAA are contained in the DA/PAA LB films. Therefore, it is likely that the two states of DA show different polymerization behaviors separately, resulting in two phases (blue and red phase). This is supported by the result that the absorption band due to the red phase is observed in the LB films of only the DA^- complexed with PAA as described below.

When $r(PAA_{unit}/DA_{total})$ is more than one, the polymerization shows different behaviors. Fig. 8(b) shows the change in UV-visible absorption spectra of the DA/PAA LB film in

group II. On irradiation with UV light, an absorption band due to red phase appears around 540 nm and develops with the irradiation time until it reaches the saturated state. However, the progress of the polymerization depends on $r(PAA_{unit}/DA_{total})$. The maximum absorbance in the saturated state decreased with the increase in $r(PAA_{unit}/DA_{total})$, which result is consistent with the expansion of the π–A isotherms at higher PAA_{unit} subphase concentrations (see Fig. 1) due to a difference in the intermolecular distance between the DA molecules. These results indicate that the difference in the π–π interaction between butadiyne groups, probably due to different arrangements, affects the morphology, resulting in different polymerization behaviors.

4. Conclusions

We have demonstrated that the polyion complex of DA and PAA is formed when PAA is introduced in the subphase. The component ratio and the ionic states of the component depend strongly on the PAA_{unit} concentration in the subphase. These phenomena have been explained by considering the salt formation, physical adsorption of PAA and the changing pH values with the varying concentration of PAA_{unit} in the subphase. The effect of the PAA_{unit} concentration on the morphology was investigated by AFM. The AFM images of a single-layer DA/PAA LB film at a PAA_{unit} subphase concentration of 0.1 mM show fingerprint-like patterns, which consist of nanofibers with a width of 30 nm and a height of 2 nm. We have demonstrated that the nanofibers are formed by globular structures. This suggests that the difference in the π–π interaction between butadiyne groups has an influence on the morphological changes, especially the formation of the nanofiber structures.

References

[1] Robert G. Langmuir–Blodgett films. New York: Plenum, 1990.
[2] Ulman A. An introduction to ultrathin organic films: from Langmuir–Blodgett to self-assembly. Boston: Academic Press, 1991.
[3] Petty MC. Langmuir–Blodgett films: an introduction. New York: Cambridge University Press, 1996.
[4] Shimomura M, Kunitake T. Thin Solid Films 1985;132:243.
[5] Higashi N, Kunitake T. Chem Lett 1986:105.
[6] Nishiyama K, Fujihira M. Chem Lett 1988:1257.
[7] Umemura J, Hishiro Y, Kawai T, Takenaka T, Gotoh Y, Fujihira M. Thin Solid Films 1989;178:281.
[8] Miyano K, Asano K, Shimomura M. Langmuir 1991;7:444.
[9] Royappa AT, Rubner MF. Langmuir 1992;8:3168.
[10] Shimomura M. Prog Polym Sci 1993;18:295.
[11] Tachibana H, Azumi R, Tanaka M, Matsumoto M, Sako S, Sakai H, Abe M, Kondo Y, Yoshino N. Thin Solid Films 1996;284:73.
[12] Hall RA, Hara M, Knoll W. Langmuir 1996;12:2551.
[13] Matsumoto M, Miyazaki D, Tanaka M, Azumi R, Manda E, Kondo Y, Yoshino N, Tachibana H. J Am Chem Soc 1998;120:1479.
[14] Niwa M, Ishida T, Kato T, Higashi N. J Mater Chem 1998;8:1697.
[15] Kawai T. J Phys Chem 1999;B103:5517.
[16] Tachibana H, Yoshino N, Matsumoto M. Chem Lett 2000:240.
[17] Clemente-Leon M, Mingotaud C, Agricole B, Gomez-Garcia CJ, Coronado E, Delhaes P. Angew Chem, Int Ed Engl 1997;36:1114.
[18] Seip CT, Granroth GE, Meisel MW, Talham DR. J Am Chem Soc 1997;119:7084.
[19] Taguchi Y, Kimura R, Azumi R, Tachibana H, Koshizaki N, Shimomura M, Momozawa N, Sakai H, Abe M, Matsumoto M. Langmuir 1998;14:6550.
[20] Tamura K, Setsuda H, Taniguchi M, Nakamura T, Yamagishi A. Chem Lett 1999:121.
[21] Tachibana H, Yamanaka Y, Sakai H, Abe M, Matsumoto M. Chem Mater 2000;3:854.
[22] Tieke B, Wegner G, Naegele D, Ringsdorf H. Angew Chem, Int Ed Engl 1976;15:764.
[23] Carlson TA. Photoelectron and Auger spectroscopy. New York: Plenum Press, 1975.
[24] Rabolt JF, Burns FC, Schlotter NE, Swalen JD. J Chem Phys 1983;78:946.
[25] Kimura F, Umemura J, Takenaka T. Langmuir 1986;2:96.